UNIVERSITY OF CALIFORNIA SAN DIEGO

Generation of a Genetic Circuit for the Spatial and Temporal Control of Cell Function

A Thesis submitted in partial satisfaction of the

requirements for the degree

Master of Science

in

Bioengineering

by

Ali Zamat

Committee in Charge:

Professor Yingxiao Wang, Chair
Professor Stephanie Fraley
Professor Jesse Jokerst

2019

The Thesis of Ali Zamat is approved, and it is acceptable in quality and form for publication on microfilm and electronically:

Chair

University of California San Diego

2019

Table of Contents

List of Figures

Acknowledgements

Firstly, I would like to thank everyone in the Wang lab. Without the constant support and depth of knowledge, this work would not be possible. I would also like to acknowledge the mentorship of Shirley Wu and the collaboration of Dr. Chi Woo Yoon for their direction in experimental design. Lastly, many thanks to Professor Wang for providing guidance and inspiration to pursue the novel and unknown.

Section 1, in part, has been submitted for publication as it may appear in Advanced Functional Materials, 2019, Zhu, Linshan; Wang, Yingxiao. The thesis author was the primary investigator and author of this paper.

Abstract of the Thesis

Generation of a Genetic Circuit for the Spatial and Temporal Activation of Cell Function

by

Ali Zamat

Master of Science in Bioengineering

University of California San Diego, 2019

Professor Yingxiao Wang, Chair

With recent advancements in gene engineering, cellular functions have been utilized in therapeutics and diagnostics in an unprecedent amount. However, biological mechanisms for many cell activities remain unknown causing various adverse effects and overall lack of control. The potency of cell therapies such as CAR-T cell therapy leads to many on-target off-tumor effects due to lack of spatial control of CAR expression within the body. To better utilize cell function as a therapeutic, diagnostic, and overall engineering tool, this work aims to generate a genetic circuit

capable of activating cell function with high spatial and temporal resolution. In utilizing clinical high-intensity focused ultrasound, localized heat can be harnessed to trigger a chemical cascade within the cell sustaining a specified gene function. Here, we demonstrate a proof of concept system in HEK293T cells where a short heat shock of 43C induces a 23% increase in the number of cells expressing a protein of interest under tightly controlled environmental conditions. We also demonstrate that 4-OHT induced ERT2 nuclear localization dominates the cytosolic retention of NFAT and a that a calcium stimulated split Cre system requires both N and C terminus of Cre as well as the calmodulin/M13 calcium induced dimerizer pair to produce functional Cre recombination. Lastly, this work characterizes the kinetics of nuclear import and export of a small NFAT library with mutations incurring variable affinities to calcineurin in an attempt to decrease system background.

1. Background and Motivation

Recent advancements in cellular engineering have provided unparalleled usage of live cells as potent therapeutics and robust diagnostics through production of genetic circuits and synthetic proteins. Of these recent advancements, Chimeric Antigen Receptor (CAR) T-Cell therapy is arguably the most successful and ground-breaking immuno-therapy for oncology. First developed in 1989[1], CARs are synthetic molecules allowing for the design and direction of T-cells for engineered control of cellular functions. A CAR molecule is typically composed of an antigen binding moiety that triggers a signaling cascade to simulate a T-cell receptor (TCR). Receptors and stimulations can be tuned and varied to produce a specified and consistent response as it allows for MHC independent binding. Essentially, CARs provide T-cells a weapon to search for and destroy the target tumor.

Such therapies have shown great success with the third generation CAR molecules. An example currently being used today is AntiCD19-CAR therapy for treating acute Lymphoblastic Leukemia (ALL) which has positive response rates greater than 80%.[2] However, high toxicities are quite prevalent in such a potent therapeutic. The most prominent toxicity induced by CAR-T therapy is cytokine release syndrome (CRS), resultant of a flood of cytokines excreted by engineered T-cells.[3] This results in a clinical syndrome of fevers, hypertension, hypoxia, and neurologic changes which need necessary intervention in as little as a couple hours after infusion.[4] Patients with CAR-T infusions must be monitored closely as such toxicities can be fatal, yet premature intervention may diminish T-cell persistence or efficacy.[4] Various organs and systems are drastically affected by CRS resulting in decreased cardiac output, acute renal injury, and hematologic variations. Neurologic toxicities resultant of high IL-2 may also occur with varied symptoms from headaches and confusion to hallucinations and seizures. Moreover, as no known

specified antigen is presented exclusively by tumor cells, various on-target, off-tumor toxicities are prevalent. For instance, healthy B-cells also express CD-19, thus, the activation of anti-CD-19 CAR-Ts to these healthy cells results in B-cell aplasia.[3] As such, a direct control of CAR-T activation is necessary to reduce side effects and increase efficacy of treatment.

With the advancements of recombinant DNA technologies and directed gene engineering, live cells can be manipulated to induce expression of native and synthetic proteins. Indeed, the manipulation of live cell genetics is evidenced by the production of insulin from *E. coli* in 1979[5] to the glycoengineered *S. cerevisiae*[6] which can produce humanized therapeutics. More recently, there is an expanding interest and feasibility in engineering CAR-T cells for precise activation. This work aims to engineer cells to respond to a clinically feasible localized stimulus in order to induce gene expression of CAR. In generating a safe, remote, and robust activation of specified gene activity, cells can be controlled to serve as potent therapeutics and engineering tools.

Section 1, in part, has been submitted for publication as it may appear in Advanced Functional Materials, 2019, Zhu, Linshan; Wang, Yingxiao. The thesis author was the primary investigator and author of this paper.

2. Creating Heat-Induced Gene Activation System

Clinical ultrasound has been utilized for over 50 years, but more recently, there has been a drastic increase to utilize ultrasound due to its non-invasive and controllable characteristics. These characteristics make it ideal to stimulate a localized “on” switch for a potent therapeutic. Localization of engineered T-cell expression of CARs at the site of tumors should reduce on-target off-tumor effects and general adverse effects of CAR expression. Generally utilized for imaging,

ultrasound typically is used in frequencies over 20kHz while medical ultrasound utilizes frequencies between 1 and 20MHz.[7] However, to induce a strong stimulation from background, High-Intensity Focused Ultrasound (HIFU) to locally heat the tumor region can be utilized. With HIFU, an ultrasound beam propagates through soft tissue with high energy frequency which is converted to heat at the focal point. HIFU can be utilized with a range of 2 to 20MHz with the depth of focus and focal size decreasing with shortened wavelength. Utilizing a frequency of 2 MHz, it is possible to generate localized heating over 80C at a penetration of 20mm with the focus incorporating an area 5mm above and below the desired depth.[8] On the other hand, At 20MHz, a group has successfully shown penetration depths from 1.7mm to 2.7mm spanning a temperature difference from 40C to 90C with a tightened focus region of 0.1-0.5mm.[9] Overall, at lower frequencies, a deeper penetration depth can be achieved while at higher frequencies, a tighter focus can be achieved. The flexibility of such a system will allow for disease specific stimuli such that the utilization of ultrasound will allow for safe and remote activation of a chemical cascade to generate gene activity. Many optogenetic systems utilize deeper penetrating red light or higher energy blue light, however, the shallow penetration of visible light through tissue incurs difficulty when attempting to stimulate deep tissue in-vivo.

Initial testing of genetic circuits will utilize heat incubation to simulate the effects of HIFU at a specified region. Cells will be engineered to convert the heat shock stimulus into a chemical cascade capable of inducing gene activation with low background and safe activation.

2.1. Generating a Chemical Cascade with TRPV1

The transient receptor potential cation channel subfamily V member 1 (TRPV1), also referred to as the “capsaicin receptor”, is a nonselective cation channel which is essential to cell signaling

mechanisms as it is sensitive and responsive to the environment.[10] It is an 838 amino acid (AA) protein consisting of six transmembrane (TM) domains and can form homomultimers or heteromultimers with TRPV2 or TRPV3.[11] As such, TRPV1 has been characterized in both open and closed structures, and characterized the channel's response to pH, ligand, and most importantly, heat.[12] More specifically, when activated by capsaicin, the Ca^{2+} to Na^{+} permeability ratio is about 10 yet heat activation yields a lower selectivity to Ca^{2+} to about 4.[11] Although slightly voltage dependent, heat induced activation was determined to be at 41.5±1.1C with a drastically steep temperature dependence and a response current independent of the number of channels present in the system.[10] The threshold temperature of TRPV1, however, is accepted to be approximately 43C at physiological resting membrane potentials of -60mV.[11] Generally found in neurons to stimulate pain sensations under noxious heat, TRPV1 channels were also found on CD4+ T cells to contribute to TCR-induced calcium signaling and downstream T-cell activation.[13] Coupled with its presence on T cells, the specificity of TRPV1 to temperatures thresholds above normal physiological conditions and selectivity towards calcium ions, make it an ideal candidate for converting a remote heat stimulus to a chemical cascade within the cell.

2.1.1. Inducing and Monitoring Calcium

The intricacies of calcium transduction in the genetic circuit are further developed in section 2.4. To best characterize stimulation, the cellular chemical response to stimulus must be monitored. This response, Ca^{2+}, can be monitored using an R-GECO calcium biosensor. R-GECO is a GCaMP-type biosensor in which a single circularly permutated fluorescent protein (cpFP) in the red channel has calmodulin (CAM) and a short calcium binding peptide (M13) bound to the C-terminal and N-terminal of the cpFP respectively.[14] The Ca^{2+} dependent binding modifies the

environment of the chromophore leading to an intensiometric increase upon Ca^{2+} changes in the cell.[14] When conducting calcium imaging experiments, the R-GECO is transiently transfected into HEK293T cells such that the cell translates the biosensor. Doing so provides live feedback of calcium levels throughout the cell upon varying stimuli.

Although best tested with heat, initial system iterations were tested with the positive control, Ionomycin, for logistic simplicity. Ionomycin is an ionophore that acts as a divalent cation transporter across the membrane with highest selectivity for Ca^{2+}.[15] It is also important to note that measurements have indicated that Ionomycin complexes and transports calcium in a one to one stoichiometry.[15]Another method to increase calcium levels in the cell is the utilization of adenosine triphosphate (ATP). ATP stimulates secretion of Ca^{2+} from the sarcoplasmic reticulum localized inositol 1,4,5-trisphosphate receptor (IP_3R) through the activation of P2Y receptors.[16] Therefore, in place of utilizing HIFU induced heat to activate the TRPV1 channel, Ionomycin and ATP will be used in preliminary experimentation to increase basal calcium levels in the cell. Nonetheless, calcium profiles under varying stimuli will be compared to ensure translation from one form to another.

2.2. Creating Gene Activation Through the Cre-Lox System

Upon conversion of a heat stimulus to a chemical signal, genetic modifications may occur to control cellular function. Common techniques include utilizing transcriptional activators or repressors such VP64 and KRAB respectively. However, to generate a sustained and powerful response, a permanent on switch must be utilized. This can be done by utilizing a Cre-loxP recombinase system. First isolated from the P1 bacteriophage, “Causing REcombination” (Cre) causes a crossing over and DNA cutting event at the “Locus of crossing over” (loxP) sequence.[17]

Cre recombinase is a 38-kDa protein from the tyrosine recombinase family that, through a series of complex biochemical reactions, creates a Cre-bound DNA duplex. This duplex is comprised of four arms bent sharply around a planar orientation of DNA sequences to allow for DNA splicing and subsequent strand exchange.[18] Essentially, to utilize this system, a DNA segment is flanked, or floxed, by the 34 base pair (bp) loxP sequence. The Cre recombinase enzyme aligns the two loxP sites and excises the interior sequence into an independent circular DNA sequence which gets degraded by natural cell mechanisms.[17]

To create a permanent response to a specified stimulus, a cell can be engineered with floxed stop codons such that Cre recombination would remove the stop codon and allow for transcription and subsequent translation of the gene after. An engineered cell can contain a floxed mCherry-STOP codon followed by a sequence encoding for CARs. The mCherry will serve as a fluorescent indicator of infection and simply serve to assist in generating a cell line while the CAR sequence remains un-transcribed as it falls after the STOP codon. For preliminary experiments, the CAR will be replaced with an eGFP so simple visualization of Cre recombination may be observed. This loxP-mCherry-STOP-loxP-eGFP sequence was infected into HEK293T cells and a cell line generated. However, simple expression of Cre will not provide the spatial and temporal control that is required to generate a therapeutic that can be flicked "on" remotely.

2.3. Induced Shuttling Through Nuclear Factor of Activated T-Cells (NFAT)

Nuclear Factor of Activated T-cells (NFAT) is a family of five transcription factors in which all but NFAT5 regulate immune responses of T-cells to induce differentiation and cytotoxicity through calcium regulation.[19] Generally, NFAT regulation is induced through increased intracellular calcium levels where calcium binds calmodulin (CM), an important transducer of

calcium signals, and activates calcineurin (CN). Briefly, CN dephosphorylates NFAT, causes translocation of the transcription factor into the nucleus, and induces genetic activation at DNA binding regions. CN recognizes and binds to two peptide sequences (PxIxIT and LxVP where x is an unspecified amino acid) flanking the NFAT regulatory domain and causes dephosphorylation of serines in the nuclear regulatory domain.[20,21] The nuclear homology region is a conserved 300 amino acid portion in which serine rich regions are phosphorylated at resting state causing NFAT localization to predominantly be in the cytosol due to exposure of a nuclear export sequence (NES). Upon dephosphorylation by CN, a nuclear localization sequence (NLS) within this region is exposed allowing for active transport of the peptide within the nucleus. Within the nucleus, the n-terminus of the peptide (Called the n-terminal trans-activation domain) is recognized by a variety of kinases such as CK1 and GSK3 phosphorylate the system and induce export.[22] Overall, it is the interplay between import and export induced through calcium which is to be harnessed to induce gene activation. However, exact conformation changes at a structural level and binding partners remain unknown[20] yet general principals have been explored. The initial system will utilize the NFATc1 fused to a Cre recombinase. The NFATc1 protein is a 716 AA peptide in which the first 417 amino acids comprise the N-terminal trans-activation domain (nTAD) and regulatory region while amino acid sequence from 418 to 716 are comprised of the DNA binding domain and c-terminal trans-activation domain(cTAD).

2.4. System Activation

A cell will be engineered to constitutively produce a fusion protein in which a Cre recombinase is attached to NFATc1 via a short GGSGGT peptide linker on its N-terminus. Due to the localization of NFAT in the cytosol, Cre activity is expected to remain low as it will remain

sequestered outside the nucleus. In activating the TRPV1 ion channel with localized heat, a transient calcium increase would activate CN. Upon CN dephosphorylation of the NHR, the Cre-NFAT fusion will be translocated into the nucleus and allow for Cre to act on the floxed gene, reducing levels of mCherry fluorescent protein and inducing GFP fluorescence. A simplified schematic of the system is visualized in Figure 1: SchematicFigure 1.

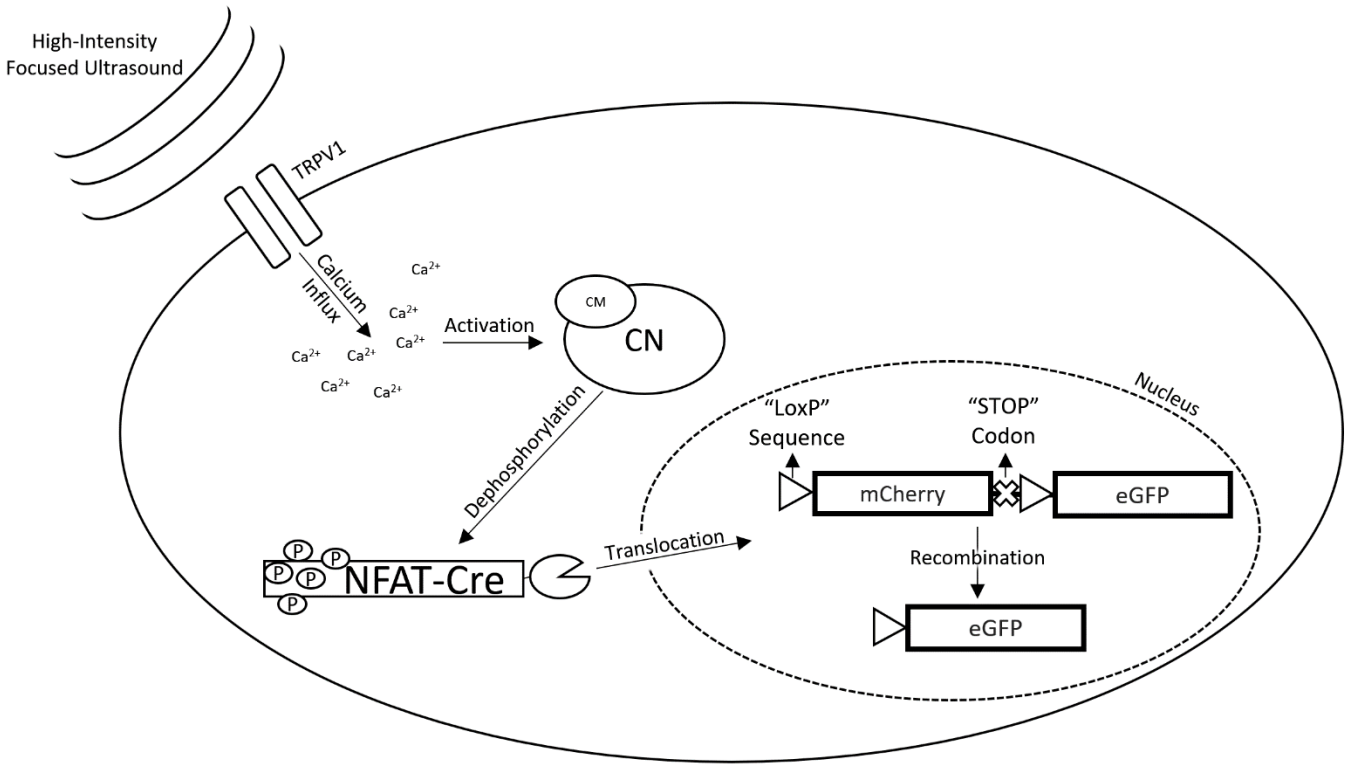

Figure 1: Schematic of genetic circuit capable of activation upon remote stimulation: HIFU causes a local temperature increase to above 43C causing an influx of Ca^{2+} ions through the TRPV1 channel. Calcium ions activate CM allowing for it to bind to CN and become catalytically active. CN dephosphorylates the NHR of NFAT leading to exposure of an NLS allowing for the translocation of the NFAT-Cre fusion protein to enter the nucleus and recombine the reporter such that eGFP is expressed.

To begin, the localization of sNFATc2 (4-460), s1NFATc1 (1-416), and s3NFATc1 (102-416) were visualized in HEK293T cells by fusing eGFP onto the C terminus of the peptide. sNFATc2 has highly characterized translocation kinetics and spans the NFATc2 regulatory region and nTAD. s1NFATc1 contains similar sections of the NFATc1 peptide in that it contains both nTAD and regulatory region. s3NFATc1, however, excludes the nTAD and is the shortest

translocation peptide tested. Calcium increases in the cell were first induced using ionomycin and ATP as a preliminary control before utilizing heat. Calcium levels were monitored using the R-GECO calcium biosensor and translocation monitored through the GFP channel. Only cells containing TRPV1, visualized through the tBFP channel, were monitored for heat experiments. From Figure 2A, we can see an induced cellular calcium increase stimulated by Ionomycin, ATP, and heat. Upon Ionomycin stimulation (left), a sharp and sustained calcium increase is observed at about a four-fold increase. This response is radically different upon ATP stimulation where an oscillatory calcium level is observed before remaining highly sustained at a similar normalized value. Lastly, upon heat stimulation through hot media perfusion, an increase is clearly observed. However, the R-GECO intensity increase is quite heterogenous among cells in similar groups which could be attributed to the variability of TRPV1 expression upon transfection. Long term imaging of cells utilizing hot media perfusion indicate cell death at about 25 minutes after addition. This physiological response is solely attributed to experimental conditions as controlled heat shock in an incubator for 30 minutes does not show significant cell death (Figure 2C, Middle). All stimuli cause an R-GECO intensity increase of three fold or greater indicating a controlled calcium increase in the cell which can generate NFAT translocation into the nucleus (Figure 2B). At resting state, GFP localization is within the cytosol as it is fused to the NFAT nuclear homology region. Upon introduction of the stimulus, GFP translocate into the nucleus within minutes. At times, GFP appears to form puncta within the nucleus, this phenomenon has not been thoroughly explored but may be attributed to cell stress as puncta generally form after long term stimulation as seen in Ionomycin and heat-treated representative images. However, while scanning the dish, a handful of cells also show this puncta morphology prior to stimulation. Upon closer inspection, the shortened NFAT still contains a small portion of the DNA binding domain and may be localizing to specific

loci within the genome. Kinetics of translocation into and out of the nucleus is quantified and characterized in section 5 below and representative images of export after ionomycin washout can be visualized in Supplemental Figure 1 for both s1NFATc1-GFP and

Figure 2: Induced calcium influx and NFAT transport. A) R-GECO calcium biosensor intensity fold change upon Ionomycin (left), ATP (middle), and heat (right) stimulation. B) Representative images portraying the import of s1NFATc1-GFP upon Ionomycin (top), ATP (middle), and heat (bottom) stimulation at 2 minutes before stimulation, 5 minutes after stimulation, and 10 minutes after stimulation. All scale bars are 12 μm in length. C) Qualitative localization of s1NFATc1-GFP localization upon 44C heat incubation for 30 minutes. Representative images of pre-heat shock and post heat shock (left, middle respectively) are quantified and tabulated in the bar graph (right). All scale bars are 48μm in length.

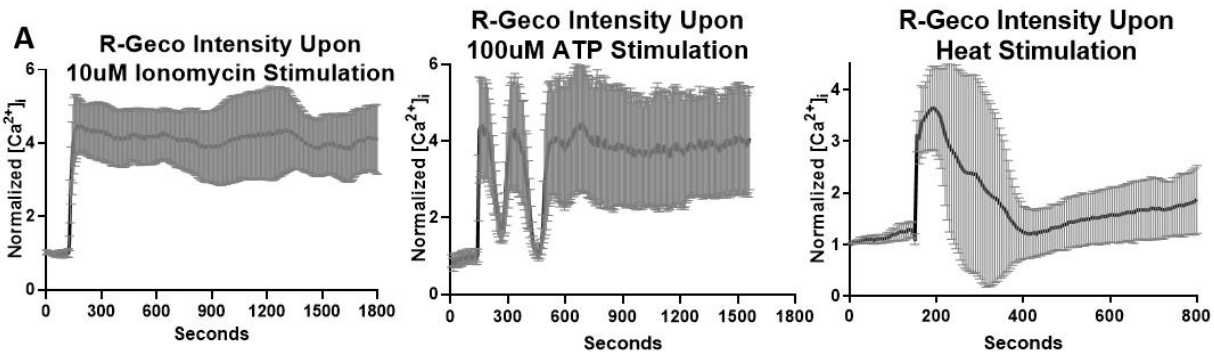
A
R-Geco Intensity Upon
10uM Ionomycin Stimulation
R-Geco Intensity Upon
100uM ATP Stimulation
R-Geco Intensity Upon
Heat Stimulation
Normalized [Ca2+]i
Seconds

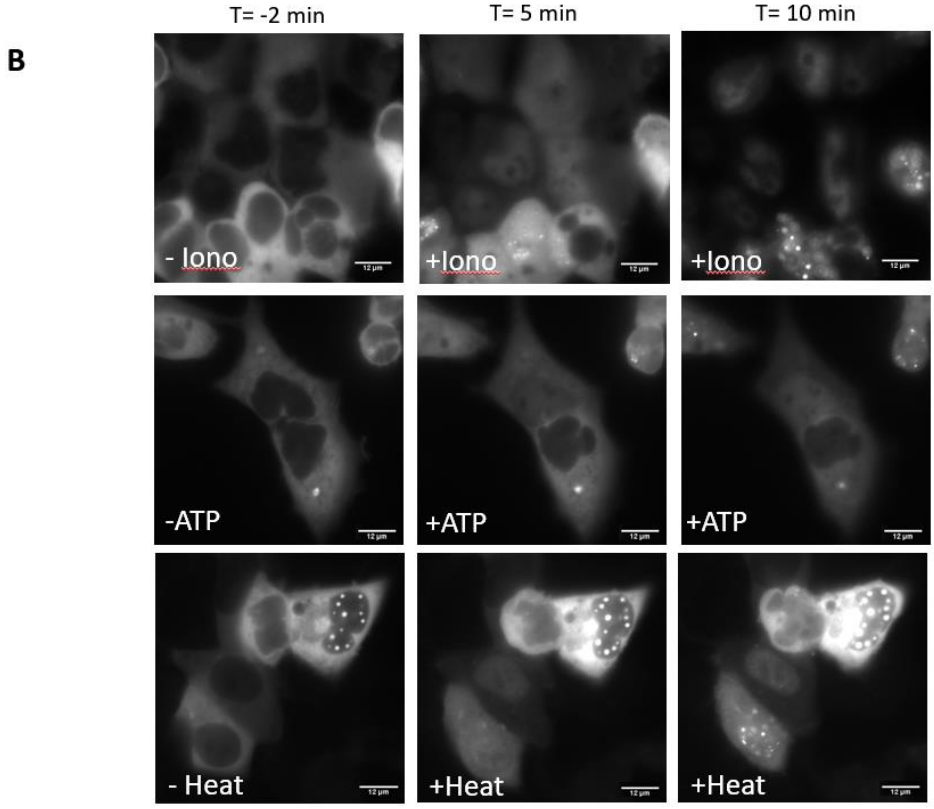
B
T= -2 min
T= 5 min
T= 10 min
- Iono
+Iono
+Iono
-ATP
+ATP
+ATP
- Heat
+Heat
+Heat

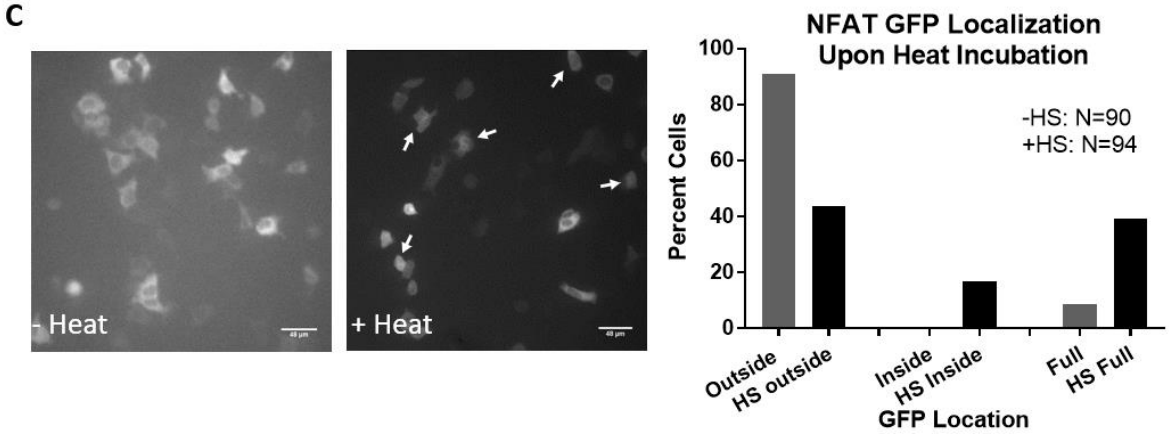
C
- Heat
+ Heat
NFAT GFP Localization
Upon Heat Incubation
-HS: N=90
+HS: N=94
Percent Cells
Outside
HS outside
Inside
HS Inside
Full
HS Full
GFP Location

s3NFATc1-GFP. To better establish this system of remote activation, translocation upon heat stimulation was further analyzed and quantified in Figure 2C. Before heat stimulation, a total of 90 cells were analyzed where 91% of cells showed clear GFP localization into the cytosol, and around 9% of cells had GFP localization throughout the cell. Prior to heat stimulation, no GFP was determined to be localized exclusively in the nucleus. However, upon incubation at 44C for 30 minutes, 94 cells were analyzed and only 43.6% showed NFAT-GFP localization exclusively in the cytosol. While around 40% were localized throughout the entire cell and 17% of cells showed localization exclusively in the nucleus. Visually, cells with complete or nuclear localization are highlighted with white arrows in a representative image in Figure 2C (Middle). As mentioned above, it is important to note that incubation at 44C does not lead to obvious cell death and will be utilized as an activation method in future experimentation. It is this translocation event that we hope to harness for genetic activation.

After induced translocation was visualized, GFP was replaced with Cre recombinase and the plasmid was transfected into a cell line expressing the LoxP-mCherry-stop-LoxP-eGFP reporter (Figure 3A). Via fluorescent microscopy the eGFP to mCherry ratio was calculated and compared to a constitutively active and diffuse Cre. To increase activation activity, s1NFATc1-cre and s3NFATc1-cre were also tested under varying conditions acting upon the same reporter cell line. Groups tested with heat were co-transfected with the TRPV1 ion channel. In order to achieve a more accurate representation of recombination, flow cytometry was utilized to gate for GFP positive cells.

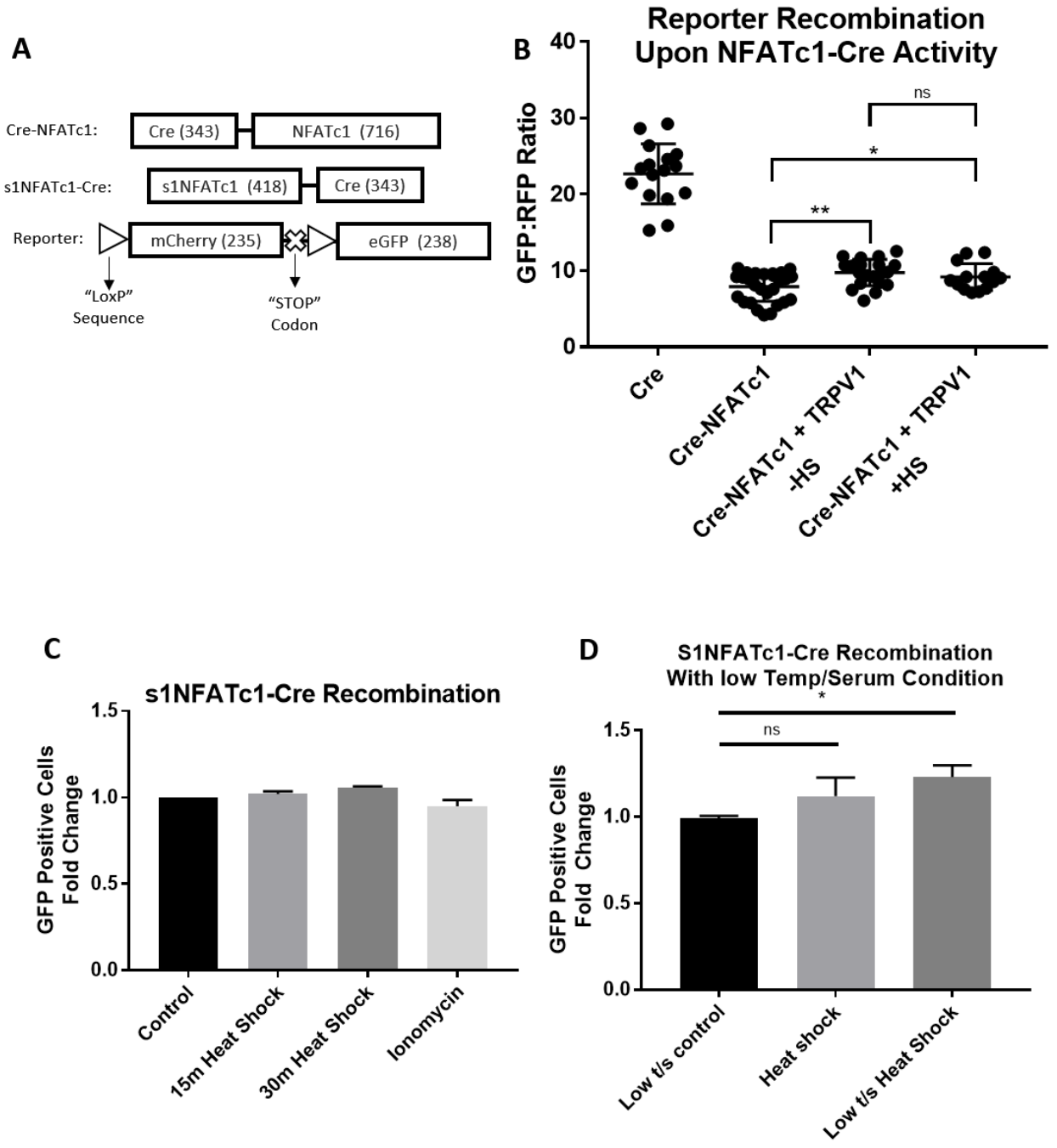

Figure 3: Induced Gene Recombination. A) Schematic of constructs generated and used with amino acid length displayed within parenthesis. B) GFP:mCherry ratio under varying conditions analyzed through fluorescent microscopy. C) GFP positive cell fold change upon varying conditions. D) GFP positive cell fold change upon preincubation in low temperature (24C) and low serum (0.5% FBS) prior to heat shock and media change.

From Figure 3B, through microscopy, the recombination event can be analyzed. Compared to a diffuse Cre, the Cre-NFAT fusion (highlighted in Figure 3A) has drastically reduced levels of

recombination indicating inactivation. When comparing the groups containing the TRPV1 channel, there is a statistically significant increase from the group without TRPV1, however; the groups treated with and without heat remain similar. Although only slightly higher than the negative control, groups with TRPV1 may lead to increased recombination due to higher calcium leakage attributed to the engineered increase of ion channels. It is hypothesized that the full Cre-NFAT may be too large to translocate into the nucleus as the fusion protein is a total size of 1059AA. To increase activation efficiency, the full length NFAT was truncated to remove the endogenous DNA binding domain and Cre moved from the n-terminus to the c-terminus (Figure 3A) to best represent the NFAT-GFP fusion protein found in literature and utilized in translocation experimentation. From Figure 3C however, we see minimal change from control groups to treated groups. Upon closer inspection of absolute values of transfection efficiencies, it appears that the s1NFATc1-Cre plasmid has high background recombination leading to a saturated, recombined reporter. This can be attributed to the fact that the recombination percentages are around 70-80% of transfection efficiencies. To further reduce background and determine efficacy of the system, the HEK293T cells were preincubated at low temperature (24C) and low serum conditions (0.5%FBS in DMEM) to effectively reduce cellular activity. From Figure 3D, there is a statistically significant, 23% increase in GFP positive cells after low temperature, low serum incubation was provided before a 44C heat shock for 30 minutes. This statistical significance from control, cannot be observed in groups treated in completed media at 37C indicating that, in fact, high background causes spontaneous translocation and subsequent recombination of the reporter sequence.

From experimentation, it is clear that a calcium response and subsequent NFAT nuclear translocation can be induced upon Ionomycin, ATP, and heat. However, it appears that the full length (1059 AA) Cre-NFATc1 fusion may not induce functional recombination while the

shortened s1NFAT-Cre (767 AA) fusion contains non-specific and spontaneous recombination. By repressing cellular activity through low temperature and low serum conditions, a statistically significant increase of 23% recombination can be observed. To further increase potency of the system as a therapeutic, the percent recombination of the control group must be further repressed.

3. Creating an AND gate with Estrogen Receptor (ERT2)

The mutated ligand binding domain of human estradiol receptor (ERT2) is highly sensitive to nanomolar concentrations of tamoxifen, or the metabolized version, 4-OHT.[23] More specifically, the mutations introduced to this estrogen receptor (ER) are G400V, M543A, and L544A and provides sharper orthogonal control over ER alone.[24] ERT2 remains sequestered in the cytosol until presented with 4-OHT which allows for strong nuclear localization. By incorporating the ERT2 sequence into on the C-terminus the s1NFATc1-Cre fusion protein, a theoretical AND gate will be produced – requiring both heat and 4-OHT to force Cre translocation into the nucleus. Due to the fact that there are two tunable motifs (NFAT and ERT2) directing translocation, the effects of varying concentrations of 4-OHT must be explored. From prior experimentation conducted in the lab, it was determined that translocation of ERT2 occurs 3 hours after treatment whereas, from above, translocation due to NFAT is achieved in minutes, thus defining the experimental timeline visualized in Figure 4D. As above, the newly constructed s1NFATc1-Cre-ERT2 will act on a fluorescent reporter to functionally express GFP upon recombination.

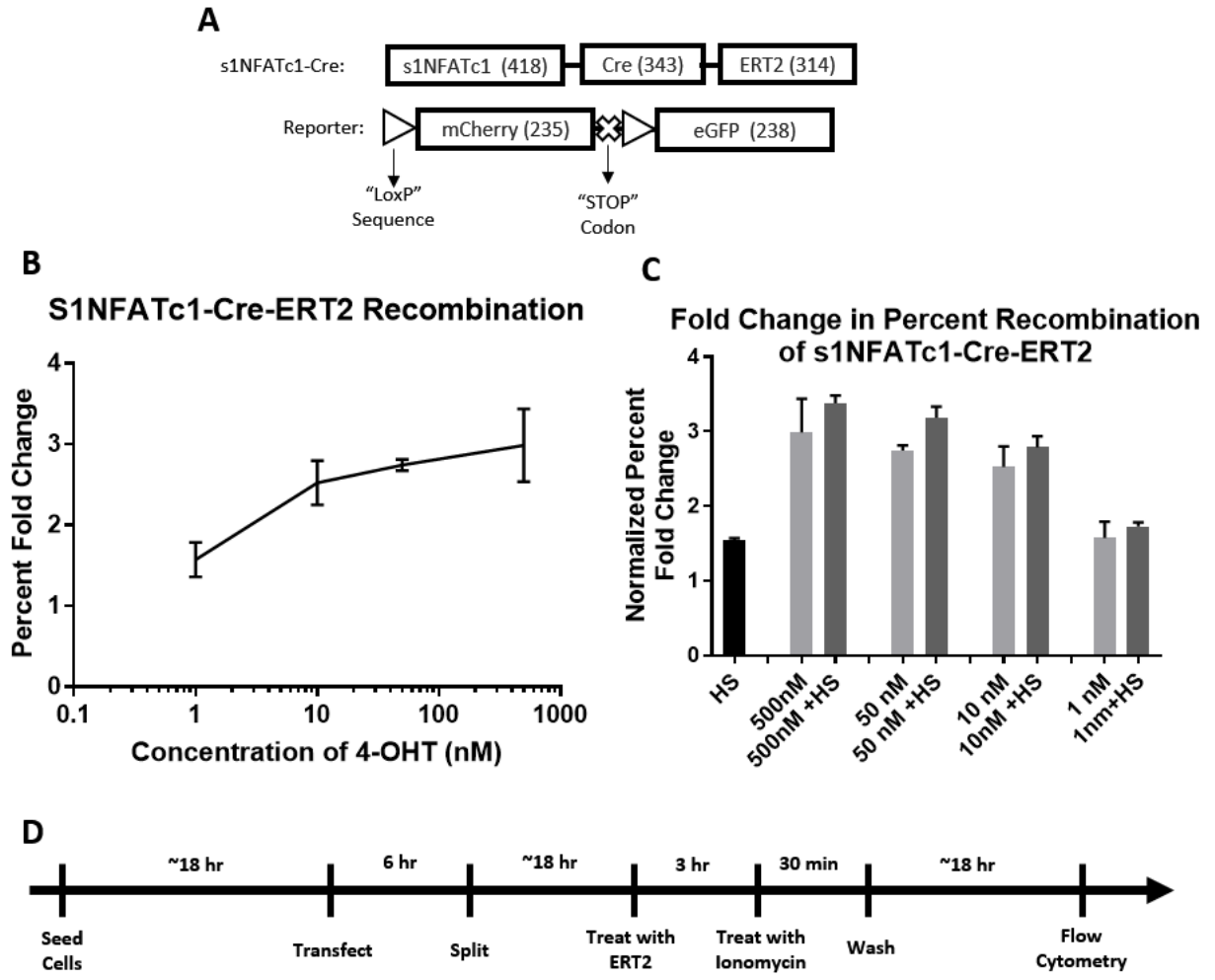

Figure 4: Effect of ERT2 on s1NFATc1 Recombination. A) Schematic of gene circuit utilized. Amino acid lengths included in parenthesis. B) Effect of 4-OHT concentrations on Cre recombination without heat. C) Effect on percent recombination of 30-minute heat shock with varying levels of 4-OHT. D) Experimental timeline for set of experiments exploring ERT2 AND gate.

From initial experimentation, the addition of 4-OHT appears to affect the percent of cells that undergo Cre recombination. From Figure 4B, the relationship between 4-OHT addition and the fold change of percent of cells that undergo recombination is logarithmic such that higher concentrations lead to increased recombination. When comparing the implementation of heat shock at varying concentrations in Figure 4C, the heat shocked groups appear to result in increased recombination for all test conditions. This indicates that there is activation of the system due to both heat and 4-OHT from 1.72-fold increase over control in the 1nM+HS group to 3.38-fold

increase in the 500nM+HS group. The fold change increase of 4-OHT treated groups to their corresponding HS treated groups, however, show minimal increases. Although providing strong temporal control upon 4-OHT stimulation, the ERT2 reduces the effect of spatial resolution and may indicate that the nuclear translocation mechanism of ERT2 overpowers that of NFAT. Therefore, moving forward, if strong spatial resolution is to be achieved, ERT2 must be decoupled from the NFAT peptide. Similar with the previous situation, however, strong uninduced recombination reduces the efficacy of the system for therapeutic purposes.

4. Reducing Background by Splitting Cre-Recombinase

To reduce the overpowering translocation activity of ERT2 when applied to NFAT, a split Cre system was utilized. By splitting the Cre, recombinase into two portions, both halves must come together and dimerize in order to functional recombination to occur. To begin, by utilizing previous literature, the Cre was split into two separate plasmids such that CreN would contain amino acids 19-59 while CreC would contain amino acids 60-343.[25] By placing these two peptides on separate plasmids, we could ensure independent expression of each peptide.

To induce dimerization of the split Cre system, the CAM/M13 dimerizer pair utilized for the R-GECO biosensor can be used. This dimerizer pair, sensitive to calcium, would allow for strong dimerization to occur upon a calcium increase. Coupled with the translocation event induced by dephosphorylated NFAT downstream of a calcium increase, creating a non-constitutive dimerization would ideally reduce background recombination observed. Overall, the short CreN segment can be fused to the s1NFATc1-M13 peptide such that upon a transient calcium increase, dimerization to the CreC-CAM would occur due to binding between and translocation will be

induced. An ERT2 can also be placed on the CreC-CAM peptide to further provide an added layer of control and to generate an AND gate as discussed above.

4.1. Utilizing the Dihydrofolate Reductase (DHFR) Degron

Since the system is experiencing high levels of uninduced background recombination, another AND gate that can be introduced is the bacterial based DHFR to act as a destabilizing peptide for our protein of interest. Through proteasomal pathways, DHFR tagged proteins will be degraded consistently until their decay is blocked by Trimethoprim (TMP), a drug that can be utilized in-vivo as it does not have any endogenous targets in mammals.[26] Within the split Cre system developed, the CreN portion can be tagged with a DHFR such that it is continually reduced. Only when TMP is supplied to the cells through cell culture media will the peptide stabilize and dimerize to the CreC portion. In doing so, the window of possible background recombination can be drastically reduced such that strong temporal control will only provide a small window for activation to occur. Although utilizing the degron will likely decrease the overall recombination percentages, the change in percent recombination between unstimulated to stimulated within the window of TMP stability could provide a background reduction that would allow for a fold change increase upon heat shock stimulation.

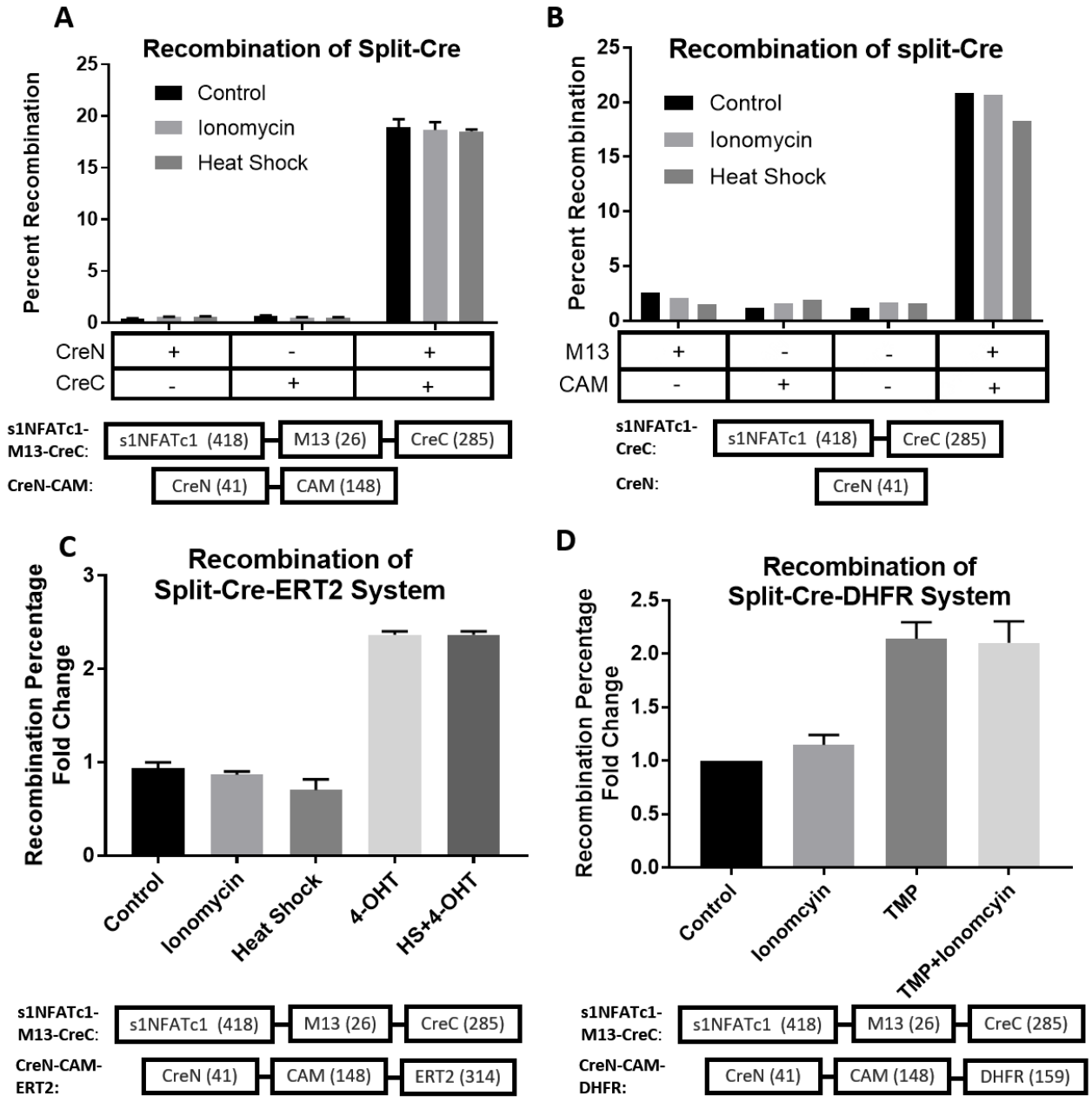

Figure 5: Recombination utilizing a calcium dimerized split-Cre system requires all components for recombination to occur. A) Analysis of recombination with varying addition of Split Cre portions. B) Analysis of recombination with varied M13/CAM dimerizer additions. Determining fold change in percent recombination with C) an ERT2 generated AND gate and D) a DHFR generated AND gate. The Split-Cre-ERT2 system was incubated with 50nM 4-OHT for 3 hours prior stimulation. The Split-Cre-DHFR system was incubated with 100μM TMP for 5.5 hours prior to stimulation. All subfigures include constructs utilized with corresponding amino acid lengths.

When determining the background recombination of the split Cre system, each component, CreN and CreC was tested individually to determine minimal necessity for functional recombination. In Figure 5A, both CreN and CreC are required for recombination to occur. Similar

to previous results, this recombination amount still shows high background recombination such that unstimulated cells show a similar increase of recombination as stimulated groups. However, the percent of cells that underwent recombination remain quite low and the signal may be attributed to leakage of the reporter. In order to determine the efficacy of the M13/CAM dimerizer, similar plasmids were made that were lacking the dimerizer pair. In Figure 5B, when only one or none of the dimerizer pair is present, recombination percentages of about 2% are observed. When both CAM and M13 are present, the recombination increases ten-fold to about 20%. This slightly higher recombination of the groups lacking the dimerizer may be attributed to spontaneous dimerization of the split Cre allowing for recombination and indicates that, in fact, that CreN, CreC, M13, CAM are required for functional recombination to occur.

Yet recombination appears to occur equally among unstimulated and stimulated groups, regardless of mode of stimulation. To reduce this, AND gates were introduced with ERT2 and the DHFR degron. The Split-Cre-ERT2 system was incubated with 50nM of 4-OHT for 3 hours prior to heat shock or ionomycin stimulation while the Split-Cre-DHFR system was incubated with 100μM TMP for 5.5 hours prior ionomycin stimulation. From Figure 5C, when applying 4-OHT a 2.4-fold change increase from control can be visualized. This increase, however, remains unaltered with the introduction of heat shock indicated that the system lacks spatial resolution. Although the ERT2 translocation is uncoupled from the translocation of NFAT, it is hypothesized that s1NFATc1-M13-CreC remains present in the nucleus at a significant level and allows for recombination to occur at high levels. Figure 5D portrays similar results in that the introduction of TMP incubation provides a 2.1-fold change increase that remains unchanged with the introduction of ionomycin after degron stabilization. Regardless of mode, when generating an AND gate

system, upon stimulation of the portion orthogonal to NFAT, significantly increased recombination occurs.

5. Controlling NFAT Translocation through Rationally Designed Mutations

Previous experimentation has shown that elucidating differences in gene expression between unstimulated and stimulated states have proven minimal. Because high gene activation occurs when compared to negative controls, it is believed that high background activity saturates the genetic reporter causing minimal change in activation. To overcome high background, a closer look the mechanism of NFAT translocation is required. As previously discussed, the NFAT NLS is exposed upon CN dephosphorylation of the regulatory region. Due to the presence of CN and kinases within the nucleus and cytosol[20] NFAT localization is in an equilibrium in which it can be found in both compartments. To further shift the resting cell to sequester engineered NFAT into the cytosol, the dissociation constant (Kd) of CN binding to the NFAT regulatory region can be altered to reduce dephosphorylation and subsequent nuclear import.

5.1. Measuring Kinetics and Characterizing Mutations

CN is involved with a series of calcium chemical cascades and, as such, interacts with various peptide sequences. Originally, the CN docking site was identified by engineering a series of NFATc2 proteins with alanine substitutions across the regulatory domain. The generated libraries elucidated the optimized and conserved PxIxIT which serves as one of two docking sites for CN.[27] By enhancing the association between CN and an engineered NFAT, it could be possible to increase sensitivity of NFAT translocation to minimal calcium increase. Generally, the PVIVIT binding sequence is accepted to have optimized affinity to CN with a dissociation constant of

0.5μM. However, as reduced sensitivity is required to decrease background, dissociation constant larger than WT must be explored. To best characterize NFATc2 translocation, a small library of CN binding sequences found in Figure 6A will be generated within the regulatory region (NFATc2 AA 4-460) and fused to eGFP. Time-lapse images of live cells under 30μM ATP stimulation and washed out through a perfusion system will be collected and analyzed. A further truncated version of the NFATc2 regulatory domain named tNFATc2 (4-399) will also be created and kinetics compared to the WT. This is done to ensure that endogenous NFAT regulation does not alter upon stimulation.

5.2. Transcriptional Activation with LexA Binding and VP64 Activation

Previous system designs utilize a genetic output achieved through Cre recombinase which accumulates background over time due to the irreversibility of recombination. To better elucidate induced activation, a transient gene reporter can be utilized. The LexA peptide is a transcriptional activator that binds to a specific DNA sequence called LexA Operator (LexO) and can cause gene activation when attached to a transcriptional activator such as VP64.[28] Due to the fact that this system is derived from bacteria, it is orthogonal to mammalian genes and should have low cross reactivity. Although creating a system responding transiently to a stimuli (until the reporter protein is degraded) poses challenges in generating a therapeutic, it may reduce the effect of calcium influx induced background recombination imposed by long term cell culture techniques.

To utilize a transient system, constructs containing NFAT with mutated CN binding domains (MxNFAT) following the order in Figure 6A will be will be fused with a LexA-VP64 sequence. In theory, at resting state, the transcriptional activator will be sequestered to the cytosol and will translocate into the nucleus upon an induced calcium increase. The LexA-VP64 will bind to a

LexO binding domain preceding a minimal promotor and mNeonGreen gene. Upon binding, VP64 will induce activation of the fluorescent mNeonGreen protein to be visualized with flow cytometry. Both reporter and transcriptional activators were transiently transfected into HEK293T cell lines.

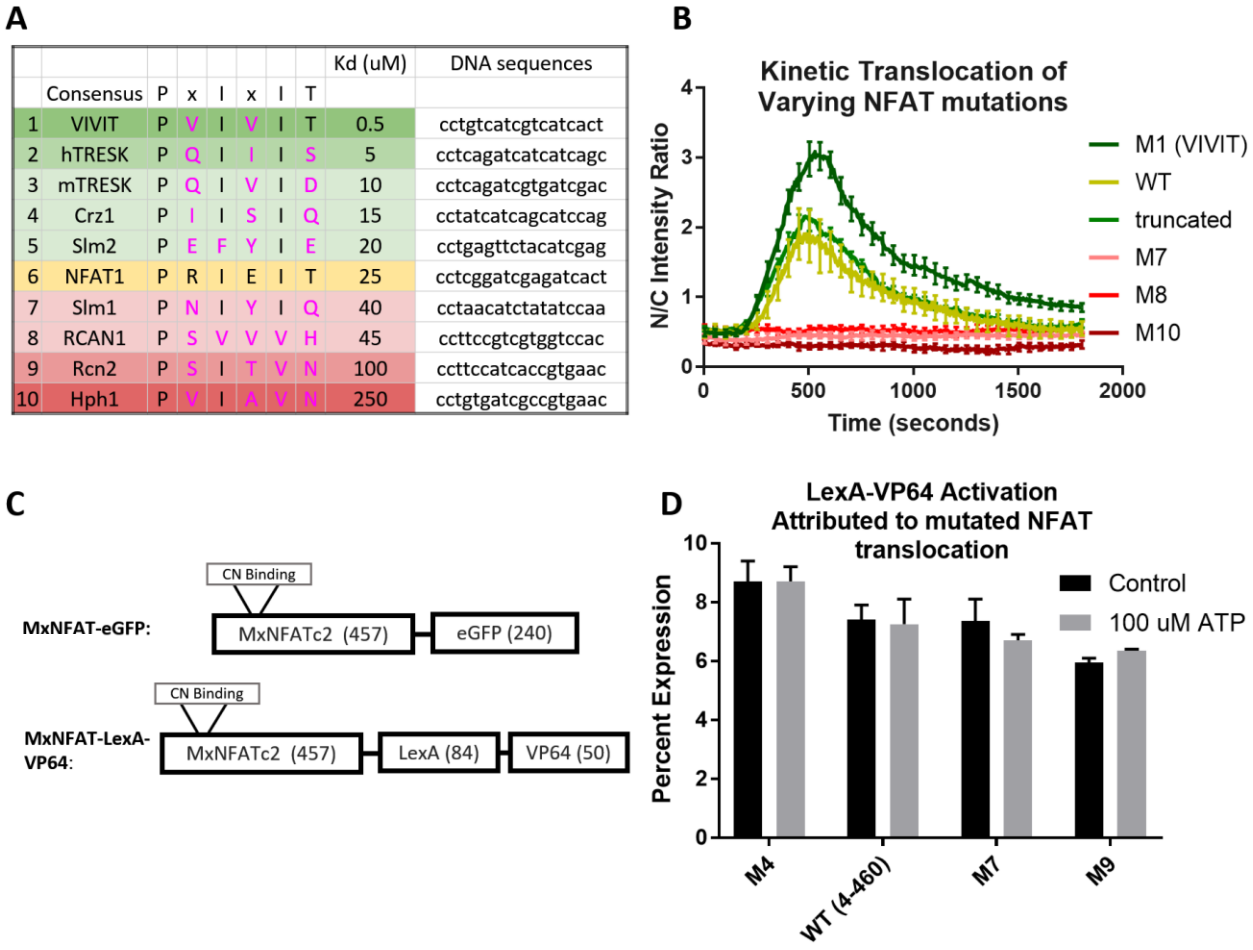

Figure 6: Effect of CN binding mutations on NFAT translocation. A) A series of mutations introduced to the CN binding domain with corresponding binding dissociation constants and DNA sequence. Table modified from Li et al.[27] B) Visualization of select translocation kinetics of MxNFAT-eGFP in which normalized nucleus intensity was divided by cytoplasmic. C) Constructs generated to visualize and induce a genetic change. Numbers in parenthesis indicate amino acid lengths D) Percent of cells with induced gene activation of mNeonGreen under varying conditions and mutations.

In generating a small library of 10 NFATc2 mutants with varying dissociation constants spanning from 0.5μM to 250μM a 500-fold difference in affinity can be explored. These mutants were generated and fused with an eGFP and LexA-VP64 as described in Figure 6C and through

live cell imaging, kinetics explored. After imaging for 120 seconds, the cells expressing the MxNFAT-eGFP constructs are perfused with 30 μM ATP and washed out 300 seconds afterwards. The fluorescent intensity ratio between the nucleus and cytoplasm were plotted across time. The WTNFAT and truncated NFAT (tNFAT) appear to translocate with similar kinetics indicated that the amino acids from 400 to 460 may not be a part of the NFAT regulatory domain. Also, it appears that the M1NFAT peptide which has highest affinity to CN can translocate more quickly with a higher ratio which is as expected. However, when reducing binding affinity to a Kd of 40μM, translocation is not observed under the same stimulus. When analyzing genetic activation of the MxNFAT-LexA-VP64 system, reporter fluorescence can be observed with all mutants tested. Further experimentation will be conducted to elucidate gene expression for all 10 NFAT mutants. Still, clear trends can be observed. M4NFAT-LexA-VP64 which has the highest binding affinity within the groups tested appears to have highest background gene expression with 8.7% of cells expressing the reporter protein. As before, no differences can be seen between induced and uninduced groups. This background, decreases to a value of 5.9% when the transcription activator has a reduced Kd to CN at 100μM. This indicates that although gene expression cannot be observed due to high background, equilibrium localization of MxNFAT is altered when CN binding sequences are changed. With higher affinity to CN, MxNFAT is more likely to be found in a dephosphorylated state and thus, induce higher gene expression while lower affinity mutants are more likely to remain in the cytosol -- reducing overall reporter gene expression. More work will be conducted to further characterize the mutant library to best understand kinetics and gene expression so that an optimal peptide sequence can be utilized.

6. Conclusions and Future Directions

The generation of a genetic circuit to allow for remote controlled cellular activation requires an in-depth look at multiple components. Firstly, upon heat stimulation, the remote signal was successfully converted to a calcium chemical response within the cell as visualized in Figure 2A. This cellular calcium increase was successfully converted to a translocation event and analyzed within Figure 2B and Figure 6B thus indicating the possibility to harness the translocation event to produce a genetic output. Under physiological conditions, the full length Cre-NFAT does not activate while the s1NFAT-Cre leads to levels of high background thus reducing the inducibility of the system. However, incubation in low temperature and low serum conditions post-transfections reduces the background levels and allows for a statistically significant 23% increase in number of cells induced to express the protein of interest. In an attempt to create fold change differences, an AND gate ERT2 peptide was fused to the c-terminus of the s1NFAT-Cre protein. Results of this system indicate that the translocation of ERT2 drastically overpowers that of NFAT allowing for temporal control of gene activation yet lacking spatial control. By splitting the Cre recombinase and inducing dimerization with the CAM/M13 dimerizer, it was successfully shown that both halves of Cre as well as both CAM and M13 are required for functional Cre to cause DNA recombination. By utilizing AND gates orthogonal to NFAT with ERT2 or DHFR, similar results were identified in that powerful temporal control can be achieved yet spatial control through a heat stimulation was reduced by the system thus indicating that the sequestration of NFAT in the cytosol was not tightly regulated and uninduced background recombination could occur within the nucleus.

To push the equilibrium of NFAT localization exclusively into the cytosol, a mutation library was made such that binding affinities to CN were altered. In fact, it was discovered that the

dynamics of translocation of the protein were altered significantly as high affinity mutants transported into the nucleus with faster kinetics and increased nuclear to cytosolic ratio whereas the opposite was true for low affinity mutants. This difference manifested itself in genetic activation as higher affinity mutants displayed increased gene activation as seen in Figure 6D. Nonetheless, despite varying background levels of gene activity, induction of the system did not provide a statistically significant change indicating that more work needs to be conducted prior to therapeutic implementation.

To begin, complete characterization of the mutant NFAT library would better elucidate the ways in which CN binding affect the equilibrium localization of the engineered NFAT. Image analysis utilizing confocal microscopy can be utilized to determine basal nuclear levels prior to induced NFAT translocation. Moreover, the implementation of the eDHFR degron must be further explored. By altering the window in which the peptide remains stable through addition of TMP, the amount of background recombination can be changed due to the degradation of CreN. Further experimentation is being conducted in which cells are preincubated with varying times of TMP prior to stimulation. Moreover, it is possible that the amount of Cre produced may saturate the reporter cell line. As such, transient transfections or virus transductions with decreased DNA amounts are used to repeat prior experiments. Overall, a decreased DNA amount and incubation time with TMP in the split-Cre-DHFR system may allow for reduced background recombination and allow for safe, remote activation of gene activity through DNA recombination.

7. Materials and Methods

7.1. DNA Construction and Cloning

All constructs were amplified to obtain important fragments through Q5 polymerase chain reaction (PCR) and assembled into a pSIN or pEGFP backbone through Gibson Assembly [New England Biolabs]. Linear DNA constructs were purified using the QIAquick Gel Extraction Kit [Qiagen]. Plasmids were amplified with DH5α bacterial cells and purified with the Miniprep Kit [Qiagen].

7.2. Cell Culture and Reagents

HEK293 cells were obtained from American Tissue Culture Collection (ATCC) [Manassas, VA], and cultured in medium containing Dulbecco's modified Eagle medium (DMEM) [Gibco], 10% fetal bovine serum (FBS) [Atlanta Biologicals, Lawrenceville, GA], and 1x penicillin/streptomycin [Invitrogen]. They were cultured in 37°C humidified-incubator with 5% CO_2. Transfections were conducted utilizing the Lipofectamine 3000 kit [Sigma Aldrich] prior to experimentation.

7.3. Image Acquisition and Analysis

Prior to imaging, glass-bottom dishes [Cell E&G] coated with fibronectin [Sigma] at a concentration of 10μg per mL and incubated at 37C for at least 30 minutes before cell plating. During imaging, HEK cells were maintained in FluoroBrite DMEM [Gibco] supplemented with 10% FBS in 37C with 5% CO_2.

7.4. flow Cytometry

Flow cytometry measurements were utilized to quantify reporter expression. Cells were resuspended in FACS wash buffer (PBS + 0.5% BSA) and processed with a BD Accuri C6

Cytometer. Data analyzed with corresponding BD Accuri system software. Data plots generated using Prism software [Graphpad]

8. Supplemental Figures

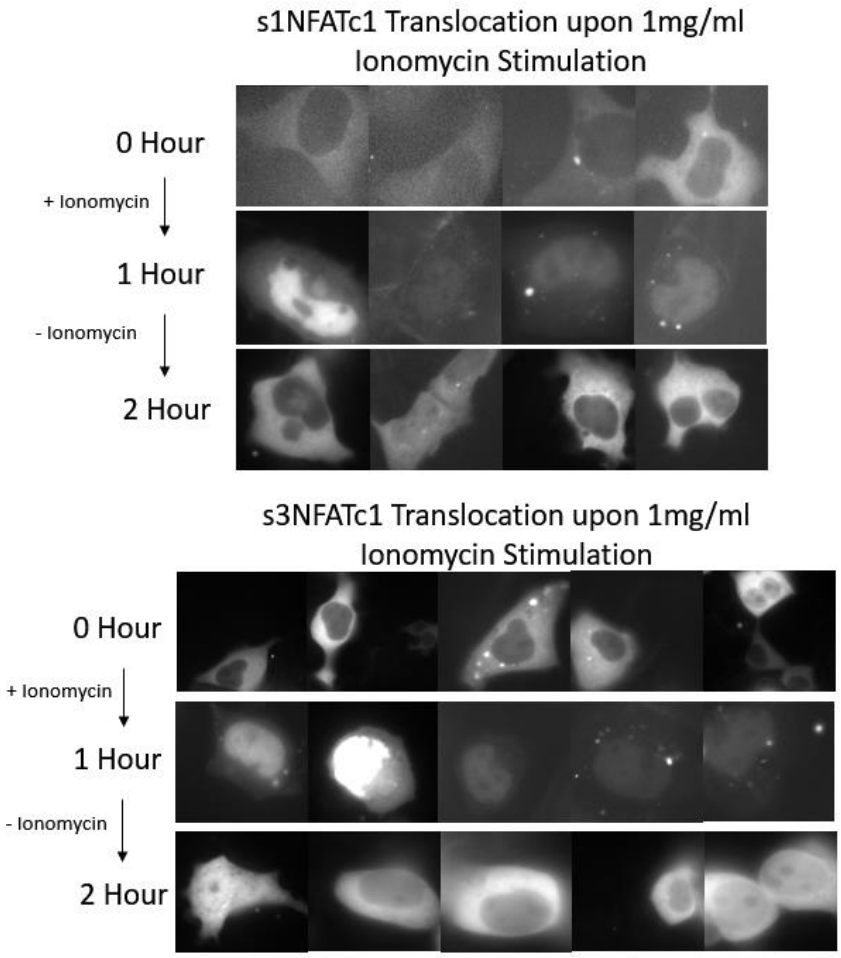

Supplemental Figure 1: Translocation response shortened NFATc1-GFP protein fusions upon incubation with and without Ionomycin.

9. References

1. Gross, G., Waks, T. & Eshhar, Z. Expression of immunoglobulin-T-cell receptor chimeric molecules as functional receptors with antibody-type specificity. *Proc. Natl. Acad. Sci.* **86**, 10024–10028 (1989).

2. Fesnak, A. D., June, C. H. & Levine, B. L. Engineered T cells: The promise and challenges of cancer immunotherapy. *Nat. Rev. Cancer* **16**, 566–581 (2016).

3. Brudno, J. N. & Kochenderfer, J. N. Toxicities of chimeric antigen receptor T cells : recognition and management. *Blood* **127**, 3321–3331 (2016).

4. Martin, B. R., Giepmans, B. N. G., Adams, S. R. & Tsien, R. Y. Mammalian cell-based optimization of the biarsenical-binding tetracysteine motif for improved fluorescence and affinity. *Nat. Biotechnol.* **23**, 1308–1314 (2005).

5. Goeddel, D. V, Kleid, D. G., Bolivar, F., Heyneker, H. L., Yansura, D. G., Crea, R., Hirose, T., Kraszewski, A., Itakura, K. & Riggs, A. D. Expression in Escherichia coli of chemically synthesized genes for human insulin. *Proc. Natl. Acad. Sci. U. S. A.* **76**, 106–110 (1979).

6. Fidan, O. & Zhan, J. Recent advances in engineering yeast for pharmaceutical protein production. *RSC Adv.* **5**, 86665–86674 (2015).

7. Pan, Y., Yoon, S., Zhu, L. & Wang, Y. Acoustic mechanogenetics. *Curr. Opin. Biomed. Eng.* **7**, 64–70 (2018).

8. Martínez-Valdez, R., Ramos Fernández, A., Vera Hernandez, A. & Leija Salas, L. Design of a low power hybrid HIFU applicator for haemostasis based on acoustic propagation modelling. *Int. J. Hyperth.* **32**, 121–131 (2016).

9. Bove, T., Zawada, T., Serup, J., Jessen, A. & Poli, M. High-frequency (20-MHz) high-intensity focused ultrasound (HIFU) system for dermal intervention: Preclinical evaluation in skin equivalents. *Ski. Res. Technol.* **25**, 217–228 (2019).

10. Cao, E., Cordero-Morales, J. F., Liu, B., Qin, F. & Julius, D. TRPV1 Channels Are Intrinsically Heat Sensitive and Negatively Regulated by Phosphoinositide Lipids. *Neuron* **77**, 667–679 (2013).

11. *Transient Receptor Potential (TRP) Channels*. (Springer, 2007).

12. Voets, T., Droogmans, G., Wissenbach, U., Janssens, A., Flockerzi, V. & Nilius, B. The principle of temperature-dependent gating in cold- and heat-sensitive TRP channels. *Nature* **430**, 748–754 (2004).

13. Bertin, S., Aoki-Nonaka, Y., de Jong, P. R., Nohara, L. L., Xu, H., Stanwood, S. R., Srikanth, S., Lee, J., To, K., Abramson, L., Yu, T., Han, T., Touma, R., Li, X., González-Navajas, J. M., Herdman, S., Corr, M., Fu, G., Dong, H., Gwack, Y., Franco, A., Jefferies, W. A. & Raz, E. The ion channel TRPV1 regulates the activation and proinflammatory properties of CD4+ T cells. *Nat. Immunol.* **15**, 1055–1063 (2014).

14. Wu, J., Prole, D. L., Shen, Y., Lin, Z., Gnanasekaran, A., Liu, Y., Chen, L., Zhou, H., Chen, S. R. W., Usachev, Y. M., Taylor, C. W. & Campbell, R. E. Red fluorescent genetically encoded Ca 2+ indicators for use in mitochondria and endoplasmic reticulum . *Biochem. J.* **464**, 13–22 (2014).

15. Hermann, T. E. Characterization of Ionomycin as a Calcium Ionophore. *J. Biol. Chem.* 5892–5894 (1978).

16. Ito, N., Ruegg, U. T. & Takeda, S. ATP-induced increase in intracellular calcium levels and subsequent activation of mTOR as regulators of skeletal muscle hypertrophy. *Int. J. Mol. Sci.* **19**, 1–15 (2018).

17. McLellan, M. A., Rosenthal, N. A. & Pinto, A. R. Cre-loxP-Mediated Recombination: General Principles and Experimental Considerations. *Curr. Protoc. Mouse Biol.* **7**, 1–12 (2017).

18. Duyne, G. D. Van. A S TRUCTURAL V IEW OF Cre-loxP S ITE -S PECIFIC R ECOMBINATION. *Annu. Rev. Biophys. Biomol. Struct.* **1**, 87–104 (2001).

19. Macian, F. NFAT proteins: Key regulators of T-cell development and function. *Nat. Rev. Immunol.* **5**, 472–484 (2005).

20. Hogan, P. G., Chen, L., Nardone, J. & Rao, A. Transcriptional regulation by calcium, calcineurin. *NFAT. Genes Dev.* **17**, 2205–2232 (2003).

21. Liu, J. O., Nacev, B. A., Xu, J. & Bhat, S. It Takes Two Binding Sites for Calcineurin and NFAT to Tango. *Mol. Cell* **33**, 676–678 (2009).

22. Okamura, H., Garcia-Rodriguez, C., Martinson, H., Qin, J., Virshup, D. M. & Rao, A. A Conserved Docking Motif for CK1 Binding Controls the Nuclear Localization of NFAT1. *Mol. Cell. Biol.* **24**, 4184–4195 (2004).

23. Hirrlinger, J., Requardt, R. P., Winkler, U., Wilhelm, F., Schulze, C. & Hirrlinger, P. G. Split-CreERT2: Temporal Control of DNA recombination mediated by split-cre protein Fragment Complementation. *PLoS One* **4**, 2–9 (2009).

24. Feil, S., Valtcheva, N. & Feil, R. Inducible Cre Mice. in *Gene Knockout Protocols: Second Edition* (eds. Wurst, W. & Kühn, R.) 343–363 (Humana Press, 2009). doi:10.1007/978-1-59745-471-1_18

25. Hirrlinger, J., Scheller, A., Hirrlinger, P. G., Kellert, B., Tang, W., Wehr, M. C., Goebbels, S., Reichenbach, A., Sprengel, R., Rossner, M. & Kirchhoff, F. Split-Cre complementation indicates coincident activity of different genes in vivo. *PLoS One* **4**, 1–10 (2009).

26. Sando, R., Baumgaertel, K., Pieraut, S., Torabi-Rander, N., Wandless, T. J., Mayford, M. & Maximov, A. Inducible control of gene expression with destabilized Cre. *Nat. Methods* **10**, 1085–1088 (2013).

27. Li, H., Rao, A. & Hogan, P. G. Interaction of calcineurin with substrates and targeting proteins. *Trends Cell Biol.* **21**, 91–103 (2011).

28. Yagi, R., Mayer, F. & Basler, K. Refined LexA transactivators and their use in combination with the Drosophila Gal4 system. *Proc. Natl. Acad. Sci.* **107**, 16166 LP – 16171 (2010).